

A COMPARATIVE STUDY OF PLATONIC SOLID LOUDSPEAKERS AS DIRECTIVITY CONTROLLED SOUND SOURCES

*Alexander Mattioli Pasqual
José Roberto de França Arruda*

Faculty of Mechanical Engineering
State University of Campinas
Rua Mendeleiev 200
13083-970, Campinas – SP, Brazil
[pasqual, arruda]@fem.unicamp.br

Philippe Herzog

Laboratory of Mechanics and Acoustics
National Center for Scientific Research
31 chemin Joseph-Aiguier
13402 Marseille cedex 20 France
herzog@lma.cnrs-mrs.fr

ABSTRACT

Compact spherical loudspeaker arrays in the shape of Platonic solids have been used as directivity controlled sound sources. Such devices are commonly used to synthesize spherical harmonic (SH) radiation patterns, which might be later combined to produce different directivities. The SH synthesis presents two main difficulties whose extent depends on the Platonic solid used: large synthesis error at high frequencies due to spatial aliasing and huge membrane velocities at low frequencies due to low radiation efficiency. This work presents a comparative theoretical study of the five Platonic loudspeakers. Their ability to reproduce SHs and the radiation efficiencies of their acoustic radiation modes are evaluated. It is shown that the dodecahedron presents the best compromise between complexity of the controllable patterns, number of channels and sound power.

1. INTRODUCTION

Compact spherical arrays of independent loudspeakers operating at the same frequency range have been used as directivity controlled sound sources. The transducers are usually distributed over the spherical frame according to a Platonic solid geometry to obtain a highly symmetrical configuration, so that the occurrence of preferred regions in the 3-D rendition space is reduced.

Hexahedral [1], dodecahedral [2, 3] and icosahedral [4] sources with one driver per face have been reported in the literature (an icosahedron with six drivers per face was proposed in [5]). Such devices are commonly used to synthesize pure spherical harmonics (SHs) in the far-field under free-field conditions, which might be later combined to produce different directivities.

The synthesis of pure SHs by a compact loudspeaker array presents two main difficulties, namely, spatial aliasing in the high-frequency range and low radiation efficiency in the low-frequency range. The former degrades the SHs synthesis [1, 2, 6] and the latter implies huge membrane velocities in order to produce meaningful sound power levels [7]. The extent of these problems is greatly affected by the position of each driver on the array and by the number of transducers, i.e., the choice of the Platonic solid is of major importance to the array performance.

Instead of using SHs as preprogrammed basic directivities, the acoustic radiation modes (ARMs) of the loudspeaker array can be used as a basis for directivity representation [7]. The

ARMs are real orthogonal functions (or vectors, if the vibrating body possesses a finite number of degrees of freedom) describing velocity patterns over the surface of a vibrating body. As far as compact loudspeaker arrays are concerned, one of the main advantages of the ARMs over the SHs is that they span a finite dimension subspace (the subspace dimension is the number of drivers in the array) on which any radiation pattern the loudspeaker array is able to produce can be projected with no approximation error, whereas SHs span an infinite dimension subspace so that truncation error generally arises. On the other hand, unlike the ARMs, the SHs lead to a directivity format that does not depend on the reproduction device and therefore the sound material so encoded is compatible to different loudspeaker arrays [8].

In fact, the real SHs are the ARMs of the continuous sphere [9], which is defined here as the sphere able to assume any surface velocity pattern (infinite number of degrees of freedom). Moreover, at low frequencies, the ARMs of spherical arrays give rise to far-field radiation patterns that match the real SHs, although the radiation efficiencies of an ARM and its corresponding SH are different [7]. In other words, at low frequencies, the synthesis error in mimicking a given target directivity in the far-field remains unchanged whether the ARMs or the SHs are used. However, only the ARMs provide the correct radiation efficiencies associated to each channel of the loudspeaker array.

This work presents a comparative theoretical study of the five Platonic solid loudspeakers (with one driver per face) as directivity controlled sound sources. Their radiation patterns are derived analytically by approximating each driver as a convex spherical cap that oscillates with a constant radial velocity amplitude over its surface, as described in [6]. The ability of the Platonic sources in reproducing pure SH patterns in the least-squares sense is reviewed. In addition, the radiation efficiencies of the ARMs of each Platonic source are computed in order to evaluate the low-frequency constraint mentioned before.

2. THEORY

This section gives an overview of the main theory related to the radiation control by a compact spherical loudspeaker array.

2.1. Acoustic radiation modes (ARMs)

This subsection presents a short introduction to the ARMs. For further details, refer to [7, 9].

This work was sponsored by CAPES (Brazil) and CNRS (France).

For a vibrating body with L degrees of freedom, the ARMs form a set of L real orthogonal vectors that span the subspace of the achievable velocity patterns over the body surface. The ARMs can be obtained by the eigenvalue decomposition of an operator related to the radiation efficiency of the vibrating body.

The radiation efficiency, σ , of a vibrating structure with L degrees of freedom can be written as

$$\sigma(\mathbf{u}) = \frac{\mathbf{u}^H \mathbf{C} \mathbf{u}}{\mathbf{u}^H \mathbf{V} \mathbf{u}} \quad (1)$$

where \mathbf{u} is a column vector of velocity amplitude coefficients, \mathbf{C} is an $L \times L$ real symmetric matrix which couples the power radiated by the elements of \mathbf{u} , \mathbf{V} is an $L \times L$ real positive diagonal matrix which leads to the spatial mean-square velocity on the structure surface and the superscript H indicates the complex conjugate transpose. Throughout this work, unless otherwise specified, lower case bold letters indicate vectors, while upper case bold letters indicate matrices.

Notice that the radiation efficiency is in the form of the generalized Rayleigh quotient. Thus, the solution of the generalized eigenvalue problem $\mathbf{C}\psi = \lambda\mathbf{V}\psi$ leads to a set of L real orthogonal eigenvectors $\psi_1, \psi_2, \dots, \psi_L$ corresponding to real eigenvalues, ordered as $\lambda_1 \geq \lambda_2 \geq \dots \geq \lambda_L$. These eigenvectors are the ARMs and the eigenvalues are their radiation efficiency coefficients, i.e., $\sigma_l \equiv \sigma(\psi_l) = \lambda_l$.

It can be shown that these modes (ARMs) radiate sound energy independently, i.e., the total radiated sound power is given by a linear combination of the sound power produced by each mode. Because such a modal decomposition is closely related to the radiation efficiency of the vibrating body, it permits ranking the expansion terms (ARMs) with respect to their radiation efficiencies, so that a reduced number of active channels can be obtained by not driving inefficient modes. In addition, the ARMs are only a function of frequency, the radiating structure geometry and the constraints the body is subjected to; they do not depend on the source of excitation and on the mass and stiffness of the structure. Furthermore, the ARMs of some radiators (e.g., a continuous sphere) are proven to be frequency independent. For these reasons, the ARMs are a useful representation of vibration patterns when one is mainly interested in the sound field radiated by a vibrating structure.

2.2. Continuous sphere

Before considering the spherical loudspeaker arrays, it is helpful to investigate some acoustical aspects of the sound field radiated by a “continuous sphere”, which was defined in section 1.

It was demonstrated in [9] that the real-valued SHs are the ARMs of the continuous sphere. In this case, since the vibrating body has an infinite number of degrees of freedom, the ARMs are functions rather than vectors. Moreover, there is an exact correspondence between each ARM and the radiation pattern it produces, which means that when the surface velocity distribution over the sphere matches a given SH function, the angular distribution of the radiated sound pressure field is also given by the same SH, regardless of frequency. Such a correspondence does not hold for the spherical loudspeaker arrays.

Let $n \in \mathbb{N}$ and $m \in \mathbb{Z} : |m| \leq n$ index the SHs. Then, the radiation efficiencies of the ARMs (SHs) are given by [7]

$$\sigma_{mn} = \left((ka)^2 \frac{dh_n^{(1)}(ka)}{d(ka)} \frac{dh_n^{(2)}(ka)}{d(ka)} \right)^{-1} \quad (2)$$

where $mn = n^2 + n + 1 + m$ is used for linear indexing of the SHs, k is the wave number, a is the sphere radius and $h_n^{(1,2)}(\cdot)$ are the spherical Hankel functions of the first and second kind.

Equation (2) shows that σ_{mn} does not depend on m and is only a function of the non-dimensional parameter ka for SHs of a given order n . The radiation efficiencies for the first 49 ARMs (SHs up to order $n = 6$) are presented in Fig. 1.

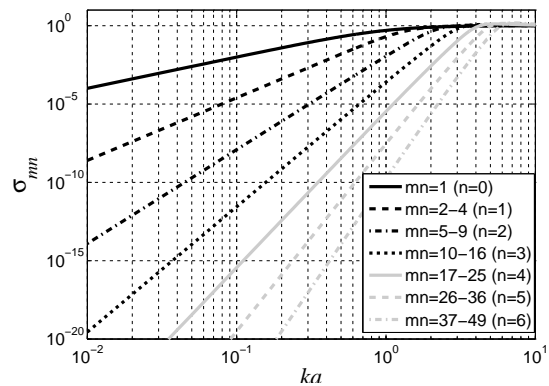


Figure 1: Radiation efficiencies of the first 49 acoustic radiation modes of the continuous sphere (spherical harmonics).

Figure 1 illustrates the grouping characteristic of the acoustic radiation modes discussed in [9]. The number of modes within each group is $2n+1$, i.e., 1 ($n = 0$), 3 ($n = 1$), 5 ($n = 2$), 7 ($n = 3$), 9 ($n = 4$), etc. It is shown that σ_{mn} increases with ka and decreases with n . Moreover, at low ka values, the radiation efficiency is strongly affected by n , so that simple directivity patterns (lower order SHs) radiate much more efficiently than complex ones. This result pinpoints the main difficulty concerning sound radiation reproduction in the low-frequency range: the sphere surface must present a huge velocity amplitude in order to produce complex directivity patterns with meaningful sound power levels.

It is worth noting that σ_{mn} can be increased over a given frequency range by increasing a . However, for compact spherical loudspeaker arrays, it is known that a larger sphere limits the radiation control in the high-frequency range due to spatial aliasing artifacts. Therefore a compromise must be sought between low and high frequency reproduction.

2.3. Discrete sphere

Some attempts have been made to predict the interaction of the radiated sound fields produced by the independent drivers of a compact spherical loudspeaker array [2, 3, 6, 7, 10]. For the moment, the spherical caps approach proposed in [6] is the most elaborate radiation prediction model for a spherical array, in which the drivers of the array are modeled as convex spherical caps, each one oscillating with a constant radial velocity amplitude over its surface. This model presents the advantage of having an analytical solution and is inspired in a previous work dealing with a single driver mounted on a rigid sphere [11].

In this work, the radiation patterns of compact spherical loudspeaker arrays are evaluated by using the spherical caps approach mentioned above, which is briefly reviewed in this subsection (for further details, refer to [6, 7]). Here, this model is called “discrete sphere”, in contrast to the “continuous sphere” considered in the previous subsection.

Let (r, θ, ϕ) be, respectively, the radial coordinate, the zenith angle and the azimuth angle. Under free-field conditions, an oscillating spherical cap placed at the north pole of a rigid sphere yields an axisymmetric sound pressure field given by [12]

$$\hat{p}(r, \theta) = \sum_{n=0}^{\infty} A_n h_n^{(1)}(kr) P_n(\cos \theta) \quad (3)$$

where $P_n(\cdot)$ is the Legendre polynomial and

$$A_n = \frac{\iota \rho c u}{2 \frac{dh_n^{(1)}(ka)}{d(ka)}} [P_{n-1}(\cos \theta_0) - P_{n+1}(\cos \theta_0)] \quad (4)$$

where $\iota = \sqrt{-1}$, ρ is the fluid density, c is the sound speed, u is the radial velocity amplitude over the cap surface and θ_0 is the half aperture angle of the cap.

By superimposing the radiated fields from L caps distributed over a rigid sphere and truncating the series given in (3) at $n = N$, the sound pressure and the radial acoustic velocity generated by a spherical array become [7]

$$p(r, \theta, \phi) = \mathbf{u}^T \mathbf{B}^T(r) \mathbf{y}(\theta, \phi) \quad (5)$$

and

$$v(r, \theta, \phi) = \mathbf{u}^T \mathbf{E}^T(r) \mathbf{y}(\theta, \phi) \quad (6)$$

where \mathbf{u} is a column vector containing the velocities of the L caps, the superscript T indicates the transpose and \mathbf{y} is a vector that contains $(N+1)^2$ complex-valued SHs, so that $y_{mn}(\theta, \phi) \equiv Y_n^m(\theta, \phi)$, with $mn = n^2 + n + 1 + m$. \mathbf{B} and \mathbf{E} are $(N+1)^2 \times L$ propagation matrices explicitly defined in [7], which depend on ka , θ_0 , ρc , kr and on the positions of the caps over the sphere.

For a discrete sphere, it can be shown that the coupling matrix introduced in subsection 2.1 is given by [7]

$$\mathbf{C} = \frac{r^2}{2\rho c S} \Re \left\{ \mathbf{B}^H \mathbf{E} \right\} \quad (7)$$

where S is the effective area of the vibrating surface. It can be demonstrated that \mathbf{C} is real and symmetric, as required, and that it does not depend on r and ρc .

By assuming that all spherical caps have the same area, the net vibration surface is $S = 2\pi a^2(1 - \cos \theta_0)L$. Hence, the matrix \mathbf{V} presented in subsection 2.1 becomes [7]

$$\mathbf{V} = \frac{1}{2L} \mathbf{I} \quad (8)$$

where \mathbf{I} is the identity matrix.

Finally, the ARMs of the discrete sphere and the corresponding radiation efficiencies can be obtained by substituting (7) and (8) into (1) and solving the eigenvalue problem.

Although (7) and (8) hold for any discrete sphere made up of identical spherical caps regardless of their positions over the sphere, this work deals only with discrete spheres whose caps are distributed over the sphere according to a Platonic solid geometry, i.e., the spatial orientation of each cap is made equal to the vector normal to a face of the polyhedron. Figure 2 shows the five Platonic solids and their midspheres. The midsphere of a polyhedron is a sphere which is tangent to every edge of the solid. The radius of the midsphere is called midradius. For acoustic purposes, a Platonic solid can be approximated by a sphere whose radius, a , is the polyhedron's midradius.

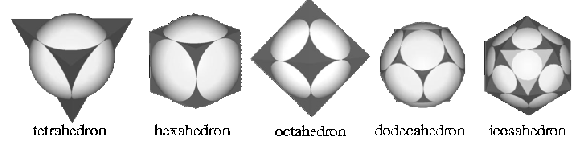


Figure 2: Platonic solids and their midspheres.

For the tetrahedron, hexahedron, octahedron, dodecahedron and icosahedron, it can be demonstrated that the upper limits of θ_0 so that the spherical caps do not overlap each other are 54.7° , 45° , 35.2° , 31.7° and 20.9° , respectively. Then, the ratio $2\pi a^2(1 - \cos \theta_0)L / (4\pi a^2)$ gives the available fraction of the spherical surface to mount the loudspeakers, namely, 84.4%, 87.9%, 73.1%, 89.5% and 65.8%, respectively. It can be noticed that, among the Platonic solids having the same midradius a , the dodecahedron presents the largest surface area available for assembling the drivers and therefore it is expected that this polyhedron will lead to the highest sound power for a given a .

2.4. Synthesis of spherical harmonics

This subsection reviews the synthesis of pure SH patterns in the far-field under free-field conditions by a compact spherical loudspeaker array. For an in-depth discussion, refer to [2, 6, 7, 8].

Since the synthesized SHs are preprogrammed basic directivities which are intended to be later combined to achieve the final desired directivity (e.g., the directivity of a musical instrument), the synthesis of each SH must take into account the spatial distribution of both its magnitude and its phase. The simplest way to perform this task is to minimize the Euclidean norm of the difference between the target SH pattern and the directivity pattern produced by the loudspeaker array, which is a well-known convex optimization problem (least-squares) whose solution can be easily found. The least-squares problem applied to the SHs synthesis with a discrete sphere is summarized in the following.

Let \mathbf{Y} be an $(N+1)^2 \times N_s$ matrix containing N_s spatial samples of the complex-valued SHs as rows (sampled version of the vector \mathbf{y}) and \mathbf{p} be a row vector containing N_s spatial samples of the sound pressure field produced by the discrete sphere evaluated at $r = r_0$, where $r_0 \gg a$ in order to ensure far-field propagation. Thus, application of (5) yields

$$\mathbf{p} = \mathbf{u}^T \mathbf{B}^T(r_0) \mathbf{Y} \quad (9)$$

By referring to (9) and letting \mathbf{Y}_{mn} be the mn -th row of \mathbf{Y} , the least-squares optimization problem can be formulated as follows, which must be solved for each frequency due to the fact that \mathbf{B} depends on the non-dimensional parameters ka and kr ,

$$\min_{\mathbf{u}} \left\| \mathbf{u}^T \mathbf{B}^T(r_0) \mathbf{Y} - \mathbf{Y}_{mn} \right\|_2 \quad (10)$$

Now, let $\mathbf{Y}^{(n)}$ be a $2n+1 \times N_s$ matrix whose rows contain spatial samples of n -th order SHs and $\mathbf{U}^{(n)}$ be an $L \times 2n+1$ matrix containing the optimum \mathbf{u} associated with each one of the $2n+1$ rows of $\mathbf{Y}^{(n)}$. So, the maximum and minimum singular values of $\mathbf{W}^{\frac{1}{2}} [\mathbf{Y}^T \mathbf{B} \mathbf{U}^{(n)} - (\mathbf{Y}^{(n)})^T]$ provide upper and lower mean square error bounds associated with the subspace spanned by SHs of order n [2, 7]. The directivity patterns associated with such bounds can be determined by examining the right-singular vectors obtained in the singular value decomposition. It is worth

noting that \mathbf{W} is an $N_s \times N_s$ diagonal matrix containing non-dimensional area weight factors applied to the spatial samples in order not to favor densely sampled regions on the sphere [7].

The singular value decomposition mentioned above can be used to evaluate the ability of a discrete sphere in reproducing target directivity patterns in the subspace spanned by SHs of a given order n , which is known to be rotation invariant [2].

3. SIMULATION RESULTS

This section presents simulation results that permit a comparison between the five Platonic loudspeakers as directivity controlled sound sources. First, the radiation efficiencies of the ARMs are evaluated, which yield a quantitative description of the low-frequency limitation of such spherical radiators. Next, the root mean square error (RMSE) in reproducing SHs are evaluated in order to take into account the spatial aliasing artifacts which degrade the directivity synthesis in the high-frequency range.

The results shown here were obtained by using the maximum θ_0 values presented in the last paragraph of subsection 2.3. Spherical caps with θ_0 as large as 54.7° and 45° are not expected to be good approximations of real driver membranes. Anyway, for the sake of convenience, such values were adopted in the simulations for the tetrahedron and hexahedron, respectively.

3.1. Radiation efficiency

The eigenvalue problem described in subsection 2.1 was carried out to obtain the ARMs of the Platonic solid loudspeakers and their radiation efficiencies — with \mathbf{C} and \mathbf{V} given by (7) and (8).

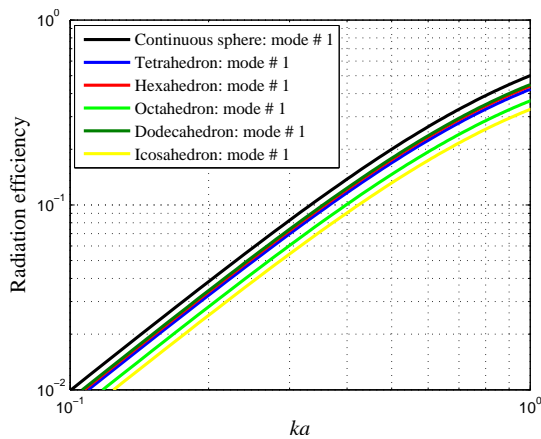


Figure 3: Radiation efficiency of the ARM # 1 of the continuous sphere and the Platonic loudspeakers.

Despite the fact that \mathbf{C} depends on ka and θ_0 , it has been observed that the eigenvalue analysis leads to the same set of L orthogonal eigenvectors regardless of the ka and θ_0 . Therefore, the results indicate that the ARMs of a discrete sphere based on a Platonic solid do not depend on ka , as is the case for a continuous sphere. On the other hand, the radiation efficiencies of the ARMs depend on θ_0 and strongly on ka . Figures 3 to 7 show the radiation efficiencies of the ARMs in the low- ka range. For comparison, the radiation efficiencies of the ARMs of the continuous sphere (SHs) shown in Fig. 1 are repeated here. The

ARMs have been arranged in descending order of their radiation efficiencies evaluated in the low- ka range.

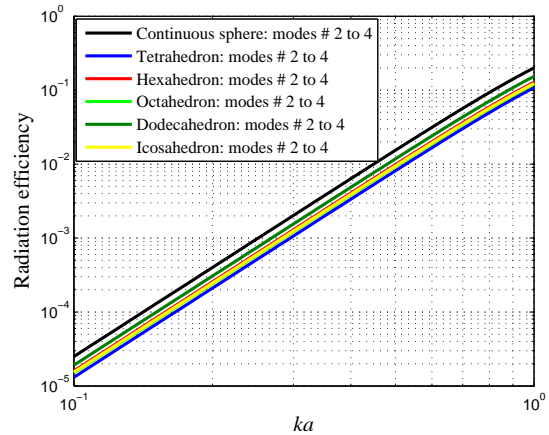


Figure 4: Radiation efficiency of the ARM # 2 to 4 of the continuous sphere and the Platonic loudspeakers.

Inspection of Figs. 3 to 7 reveals that the ARMs of the discrete spheres possess the grouping characteristic in the same way as the continuous sphere — each one of these figures corresponds to a radiation group except for Fig. 6, which presents two radiation groups for the icosahedron. The continuous and discrete sphere curves present the same behavior at low ka values and the radiation groups are well discriminated. In addition, none of the Platonic loudspeakers is able to radiate more efficiently than the continuous sphere, as expected.

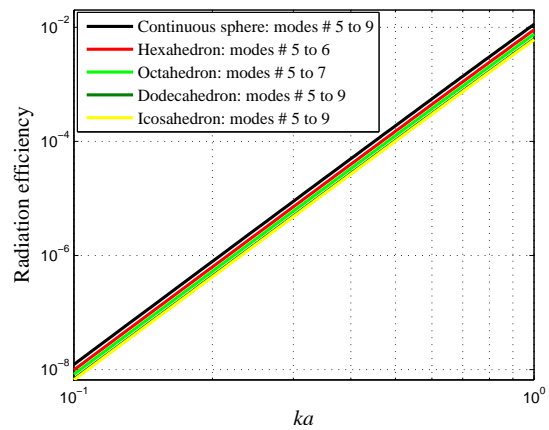


Figure 5: Radiation efficiency of the ARM # 5 to 9 of the continuous sphere, the dodecahedron and the icosahedron, as well as ARM # 5 to 6 of the cube and ARM # 5 to 7 of the octahedron.

The ARMs of the Platonic loudspeakers give rise to far-field directivity patterns that match the real-valued SHs in the low- ka range [7], which explains the similar trend of the radiation efficiency curves observed for the continuous and discrete spheres. The first radiation group (ARM # 1) yields a monopole, the second one (ARMs # 2 to 4) yields dipoles, the third one (Fig. 5) leads to 2-nd order SHs, the fourth one (Fig. 6) yields 3-rd order SHs and the fifth radiation group (Fig. 7) leads to 4-th order SHs.

Figures 3 to 7 show that the radiation efficiency curves of the Platonic loudspeakers are very similar. Thus, as far as the

sound power is concerned, the dodecahedron seems to be the best choice among the Platonic solids because it possesses the largest available surface area to mount the drivers.

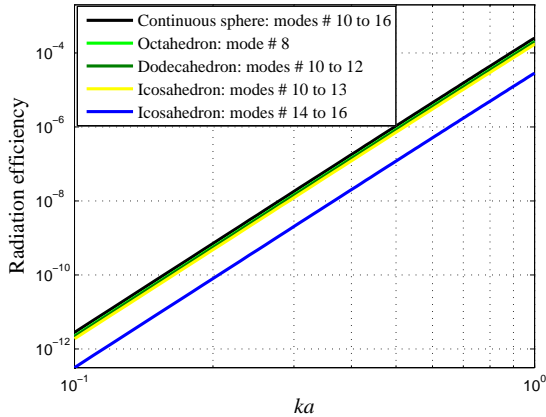


Figure 6: Radiation efficiency of the ARM # 10 to 16 of the continuous sphere, ARM # 8 of the octahedron, ARM # 10 to 12 of the dodecahedron and ARM # 10 to 16 of the icosahedron.

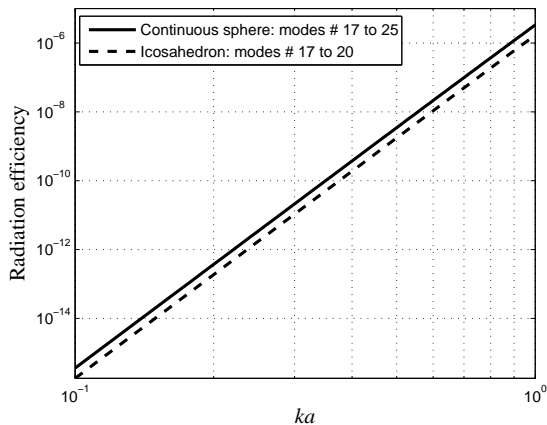


Figure 7: Radiation efficiency of the ARM # 17 to 25 of the continuous sphere and the ARM # 17 to 20 of the icosahedron.

3.2. Synthesis error

Figure 8 shows the upper and lower bounds of the RMSE that arise when synthesizing functions in the SH subspaces up to order $n = 3$ by Platonic loudspeakers. The RMSE was computed as described in subsection 2.4 by assuming the following values: $N_s = 780$, $r_0 = 10a$ and $N = 10$. For each spherical array, only one curve is presented for $n = 0$ and $n = 1$ because computations have shown that upper and lower error bounds for these subspaces are not distinguishable — the same is valid for $n = 2$ as far as the dodecahedron and the icosahedron are concerned. This means that a given directivity pattern in these subspaces can be freely rotated without affecting the RMSE. However, for $n = 3$ (and $n = 2$ for the tetrahedron, hexahedron and octahedron), the error is not uniformly distributed over the subspace, so that there are unachievable patterns and well synthesized pat-

terns; both can be determined by examining the right-singular vectors obtained in the singular value decomposition.

The RMSE rises as ka and n increases. As a rule of thumb, it is not possible to synthesize a pure SH of order $n > \sqrt{L} - 1$ due to spatial aliasing [6]. However, high order SHs might co-exist with low order ones in the radiated field from a discrete sphere. This phenomenon is also due to spatial aliasing and takes place as ka increases, leading to synthesis error as shown in Fig. 8. Such a behavior can be explained by examining the radiation efficiencies of the SHs, which were presented in Fig. 1.

Figure 1 shows that the efficiency curves of the radiation groups are well discriminated in the low- ka range, so that simple directivity patterns radiate much more efficiently than complex ones. Thus, even if the discrete sphere excites high order SHs due to spatial aliasing, they will not propagate to the far-field. Therefore, error in SH synthesis is small at low ka values provided that r_0 is made sufficiently large. On the other hand, the efficiency curves of the SHs become closer as ka increases, so that spatial aliasing produces non-evanescent undesirable patterns in the sound field, leading to synthesis error.

In order to reduce the spatial aliasing artifacts that degrade the SH synthesis at high frequencies, the sphere radius a can be made smaller. However, the low radiation efficiency at low ka values imposes a constraint on the directivity synthesis in the low-frequency range, as said before. Thus, the design of a spherical loudspeaker array for SH synthesis must be a compromise between low and high frequency reproduction.

Figure 8 reveals that the dodecahedron yields the smallest RMSE for the SH subspaces of orders $n = 0$ and $n = 1$, while it performs similarly to the icosahedron for $n = 2$. However, unlike the latter, the former is not able to provide full radiation control for $n = 3$. Nevertheless, the icosahedron's ability to synthesize functions in this subspace is limited to the low- and medium- ka ranges, and also the radiation efficiencies of its ARMs corresponding to the 3-rd order SHs are very low at low ka values, as shown in Fig. 6. Furthermore, the icosahedron gives the smallest net radiation surface among the Platonic solids, whereas the dodecahedron presents the largest one. Hence, the synthesis of functions in the subspace $n = 3$ by an icosahedral array is restricted to a narrow frequency band. Moreover, the extra eight channels that must be handled when using an icosahedron rather than a dodecahedron might be critical in real-time applications. Thus, among the Platonic solids, the simulation results indicate that the dodecahedron is the best choice for directivity control.

4. CONCLUSION

This work presented a comparative theoretical study of the five Platonic loudspeakers with one driver per face as directivity controlled sound sources. The comparison was made in terms of radiation efficiency and synthesis error, which limit radiation control at low and high frequencies, respectively.

The results indicated that the dodecahedron gives the best compromise between number of channels, sound power and complexity of the controllable patterns. Although the latter increases with the number of drivers, using more transducers does not ensure a reduction in the synthesis error for low-order SHs. In this sense, the area and shape of the vibrating surface were proven to be more important than the number of drivers.

It is worth noting that the only benefit of using more drivers per face is to provide control over some extra high-order SHs within a very limited frequency range. No significant improve-

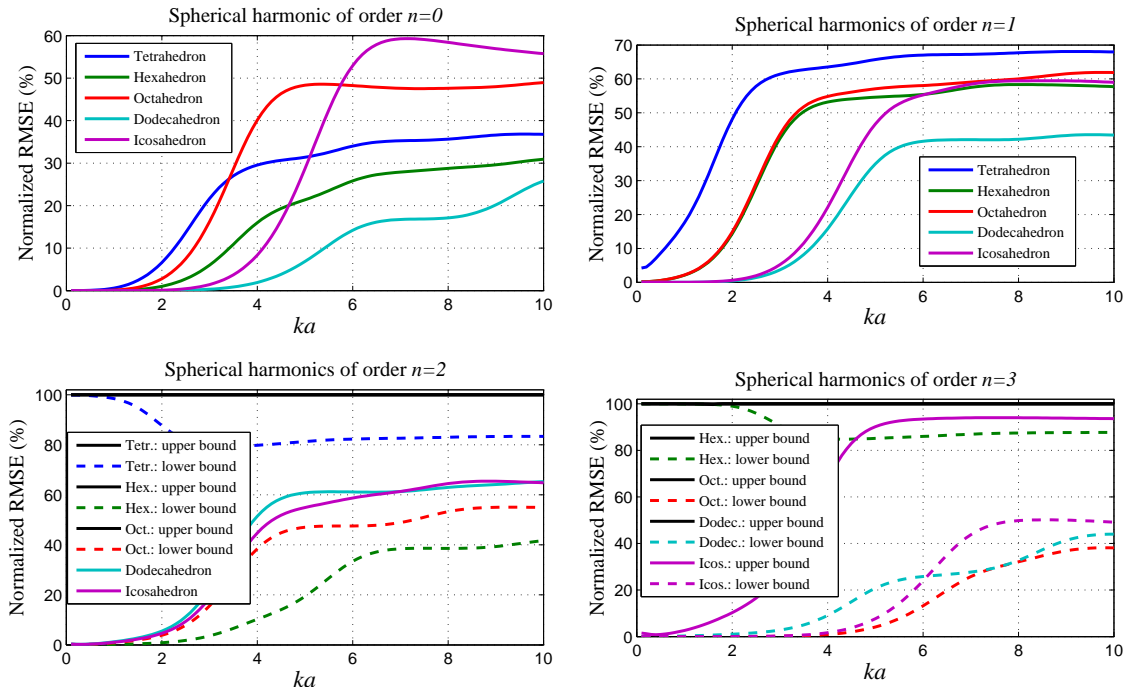


Figure 8: Upper and lower bounds of the normalized root mean square error (RMSE) achieved in the synthesis of functions in the subspaces spanned by spherical harmonics of orders 0, 1, 2 and 3.

ment either in the sound power levels or in the synthesis error for low-order SHs is expected to be achieved.

Finally, the theory presented here holds also for spherical loudspeakers other than Platonic ones. Moreover, the ARMs approach makes it possible to investigate non-spherical arrays too. In this case, the radiation patterns and the ARMs can be derived by using the boundary element method, for example.

5. ACKNOWLEDGMENT

The authors are grateful to Cédric Pinhède (UPR7051, France), Lucas Cóser (Unicamp, Brazil) and Franz Zotter (IEM, Austria).

6. REFERENCES

- [1] O. Warusfel and N. Misdariis, "Directivity synthesis with a 3D array of loudspeakers: application for stage performance," in *Proceedings of the COST G-6 Conference on Digital Audio Effects (DAFX-01)*, Limerick, Ireland, Dec. 2001.
- [2] P. Kassakian and D. Wessel, "Characterization of spherical loudspeaker arrays," in *Proceedings of the 117th Audio Engineering Society Convention*, San Francisco, CA, USA, Oct. 2004, paper number 6283.
- [3] M. Pollow and G. K. Behler, "Variable directivity for Platonic sound sources based on spherical harmonics optimization," *Acta Acustica united with Acustica*, vol. 95, no. 6, pp. 1082–1092, Nov. 2009.
- [4] F. Zotter, "Analysis and synthesis of sound-radiation with spherical arrays," PhD Dissertation, University of Music and Performing Arts, Institute of Electronic Music and Acoustics, Graz, Austria, 2009.
- [5] R. Avizienis, A. Freed, P. Kassakian, and D. Wessel, "A compact 120 independent element spherical loudspeaker array with programmable radiation patterns," in *Proceedings of the 120th Audio Engineering Society Convention*, Paris, May 2006, paper number 6783.
- [6] F. Zotter, A. Sontacchi, and R. Höldrich, "Modeling a spherical loudspeaker system as multipole source," in *Proceedings of the 33rd German Annual Conference on Acoustics*, Stuttgart, Mar. 2007.
- [7] A. M. Pasqual, J. R. d. F. Arruda, and P. Herzog, "Application of acoustic radiation modes in the directivity control by a spherical loudspeaker array," *Acta Acustica united with Acustica*, vol. 96, no. 1, pp. 32–42, Jan. 2010.
- [8] O. Warusfel and N. Misdariis, "Sound source radiation synthesis: from stage performance to domestic rendering," in *Proceedings of the 116th Audio Engineering Society Convention*, Berlin, May 2004, paper number 6018.
- [9] K. A. Cunefare, M. N. Currey, M. E. Johnson, and S. J. Elliott, "The radiation efficiency grouping of free-space acoustic radiation modes," *Journal of the Acoustical Society of America*, vol. 109, no. 1, pp. 203–215, Jan. 2001.
- [10] B. Rafaely, "Spherical loudspeaker array for local active control of sound," *Journal of the Acoustical Society of America*, vol. 125, no. 5, pp. 3006–3017, May 2009.
- [11] P. S. Meyer and J. D. Meyer, "Multi acoustic prediction program (MAPP): recent results," Meyer Sound Laboratories Inc., Tech. Rep. presented at the Institute of Acoustics (Stratford upon Avon, UK), Nov. 2000.
- [12] E. G. Williams, *Fourier Acoustics: Sound Radiation and Nearfield Acoustical Holography*. Academic Press, 1999, ch. 6, pp. 183–234.